



HAL
open science

Hole injection contribution to transport mechanisms in metal/p⁻ /p⁺⁺ and metal/oxide/p⁻ /p⁺⁺ diamond structures

Pierre Muret, David Eon, Aboulaye Traoré, Aurélien Maréchal, Julien Pernot, Etienne Gheeraert

► To cite this version:

Pierre Muret, David Eon, Aboulaye Traoré, Aurélien Maréchal, Julien Pernot, et al.. Hole injection contribution to transport mechanisms in metal/p⁻ /p⁺⁺ and metal/oxide/p⁻ /p⁺⁺ diamond structures . *physica status solidi (a)*, 2015, 212 (11), pp.2501-2506. 10.1002/pssa.201532187 . hal-01258521

HAL Id: hal-01258521

<https://hal.science/hal-01258521>

Submitted on 19 Jan 2016

HAL is a multi-disciplinary open access archive for the deposit and dissemination of scientific research documents, whether they are published or not. The documents may come from teaching and research institutions in France or abroad, or from public or private research centers.

L'archive ouverte pluridisciplinaire **HAL**, est destinée au dépôt et à la diffusion de documents scientifiques de niveau recherche, publiés ou non, émanant des établissements d'enseignement et de recherche français ou étrangers, des laboratoires publics ou privés.

Hole injection contribution to transport mechanisms in metal/p⁻/p⁺⁺ and metal/oxide/p⁻/p⁺⁺ diamond structures

P. Muret¹, D. Eon^{*1}, A. Traoré¹, A. Maréchal¹, J. Pernot^{1,2}, E. Gheeraert¹

¹ Univ. Grenoble Alpes, Inst. NEEL, F-38042 Grenoble, France
and CNRS, Inst. NEEL, F-38042 Grenoble, France

² Institut Universitaire de France, 103 Boulevard Saint-Michel, F-75005 Paris, France

Received XXXX, revised XXXX, accepted XXXX

Published online XXXX

Key words: diamond, carrier transport, electronic devices

* Corresponding author: e-mail pierre.muret@neel.cnrs.fr, Phone: +33-476-881193, Fax: +33-476-881191

Heterostructures such as Schottky diodes and metal/oxide/semiconductor structures are the building blocks of diamond electronic devices. They are able to carry large current densities, up to several kA/cm², if a heavily boron doped layer (p⁺⁺) is included in the semiconducting stack, thus affording a metallic reservoir of mobile holes close to the lightly doped layer (p⁻). In this work, hole injection effects are evidenced experimentally in the two previously mentioned devices and also simulated numerically. Although the potential barrier height at metal/semiconductor interfaces is a fundamental parameter, a more general approach consists in defining the current density from the product

of an effective velocity and carrier concentration at interface. In accordance with experimental results, such a view permits to describe both depletion and accumulation regimes, which indeed can exist at the metallic or oxide interface, and to take into account the increase of the hole concentration above the thermal equilibrium one in the p⁻ layer. The lower the temperature, the larger is this second effect. For sufficiently thin p⁻ layers, typically below 2 μm, this effect frees device operation from the limitation due to incomplete ionization of acceptors and allows a strong decrease of the specific resistance and forward losses while preserving breakdown voltages in the range 1.4 to 2 kV.

Copyright line will be provided by the publisher

1 Introduction

Diamond heterostructures show huge potentialities for high power and high temperature electronic devices due to the astounding physical and electrical properties of this semiconductor such as wide band gap ($E_G = 5.45$ eV), high thermal conductivity ($22 \text{ W} \times \text{cm}^{-1} \times \text{K}^{-1}$), room temperature mobility of holes close to $2000 \text{ cm}^2 \times \text{V}^{-1} \times \text{s}^{-1}$ and high breakdown field ($F > 7.7 \text{ MV/cm}$) as already demonstrated recently [1,2]. P-type device operation can also gain benefit from the ability of diamond to be heavily doped with boron, above the metallic conductivity limit. However, the ionization energy of boron acceptors, near 0.37 eV, induces complete ionization only around 550 K

and above in lightly doped layers, which are necessary to lower electric fields in depletion zones. Accordingly, the hole concentration is one to two orders of magnitude smaller than the acceptor concentration at room temperature, making the conductivity somewhat insufficient. With a lightly doped layer (p⁻) thicker than 10 μm, the current-voltage characteristics become strongly temperature dependent [3,4] and the specific electrical resistance hardly smaller than $1 \text{ } \Omega \cdot \text{cm}^2$ at room temperature [4]. Conversely, with a n-type layer not exceeding a few hundreds nanometers, the operation of such a Schottky p-n junction [5] becomes completely governed by carrier injection, which permits to reach several kA/cm² in the forward

Copyright line will be provided by the publisher

regime, but at the expense of a very limited breakdown voltage in the reverse regime. Here, we show that stacking a lightly doped layer (p^-) with a well designed thickness onto a heavily doped layer (p^{++}) or substrate can circumvent all these drawbacks. In lightly doped diamond layers with thicknesses up to $2 \mu\text{m}$, the heavily doped layer or substrate is able to inject holes, thus increasing the hole concentration well above the equilibrium one down to the interface with the oxide or metal, as demonstrated both experimentally and from simulation in this work. Calculations relying either on the numerical solutions of the complete basic equations set or on transport equations relevant only for holes are developed in order to attempt predicting the optimal thickness of the p^- layer. In all the structures, at sufficiently high injection level, the interface with the metal or oxide comes into accumulation regime, including the case of Schottky diodes. Hence, the diode current relies more generally on the transport model based on the majority carrier population and effective velocity at interface rather than on the potential barrier height of the junction. Finally, indications can be derived for the design of devices based on vertical and pseudo-vertical heterostructures in order to maintain an optimal trade-off between lowest forward losses, minimal specific resistance at room temperature and highest breakdown voltages.

2 Experimental transport characteristics of devices

The current-voltage characteristics of Zr/oxidized diamond diodes annealed at 450°C are firstly presented (Fig. 1) and analyzed. The diamond stack comprises a lightly doped layer, $1.3 \mu\text{m}$ thick and containing $5 \times 10^{15} \text{ B/cm}^3$, on a heavily doped layer, $0.2 \mu\text{m}$ thick and containing $(2 - 4) \times 10^{20} \text{ B/cm}^3$, epitaxially grown on a Ib substrate. More detailed properties have been already presented in [6], specially the fabrication recipes and the breakdown field in excess of 7.7 MV/cm under reverse bias, confirming older results [2]. Fair uniformity and reproducibility of the electrical characteristics of the diodes fabricated on one or several substrates have been demonstrated [6]. A complete analysis of the transport mechanisms at stake in these Schottky junctions in the depletion regime at various temperatures is currently under submission[7]. In this later study, different methods able to extract the true homogeneous potential barrier height Φ_B^{hom} , free of the random barrier lowering due to interface inhomogeneities and described by its standard deviation σ_ϕ [8,9], are demonstrated and applied. The derivation of parameters displayed in Fig. 1 is done here along three steps: (i) the derivation of σ_ϕ from the adjustment of the apparent barrier got from the current density J_s extrapolated at zero junction voltage as a function of temperature T (not shown here); secondly, the Richardson plot of J_s/T^2 corrected by the term proportional to σ_ϕ^2 shown in the inset of Fig. 1 which permits to derive the effective Richardson constant A^{**} ; thirdly, the final adjustment of

the homogeneous barrier height Φ_B^{hom} and ideality factor n (here 1.07) to the experimental current density as a function of voltage in the linear part of the characteristics plotted in a semi-logarithmic scale as in Fig. 1, taking the image force lowering $\Delta\Phi_{if}$ into account.

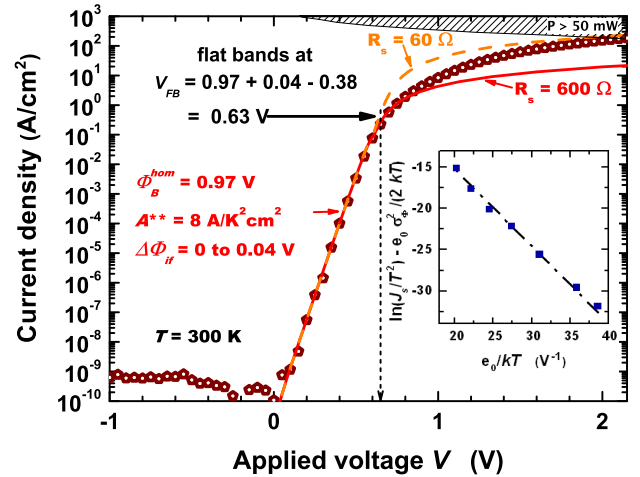


Figure 1 Experimental current density of the diode as a function of total voltage displayed with open symbols and fitting curves based on the parameters indicated on the figure and determined by the method described in the text; the Richardson plot is shown in the inset. The hatched area close to upper right corner delineates a constant dissipated power of 50 mW below which estimated self-heating remains smaller than 5K.

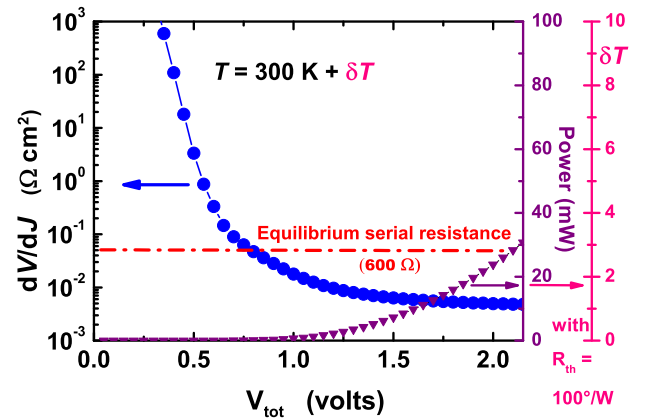


Figure 2 Specific resistance of the diode as a function of total voltage displayed with full circles. Downward triangles feature both dissipated power and temperature increase δT sketched in K on the right vertical scale.

In the present case, with an ideality factor n decreasing from 1.07 at 300 K down to 1.04 at 600 K, the homogeneous barrier height of these almost perfect junctions turns out to be $0.97 \pm 0.02 \text{ V}$, in good agreement with an other determination for Zr on oxygenated diamond [10]. Taking

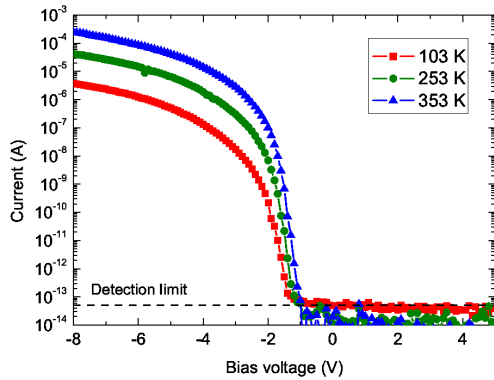


Figure 3 Current-voltage characteristics in a MOS heterostructure for several temperatures.

into account the image force effect which adds 0.04 V to the barrier at flat bands [7, 9] and the calculated energy difference between the bulk Fermi level and valence band top of 0.38 eV from data in [1], the applied voltage needed to induce flat bands amounts to 0.63 V, as indicated on Fig. 1. For larger junction voltages V , which are necessary to reach current densities J_p higher than 0.4 A/cm², band bending is inverted, the interface turns into accumulation regime and the apparent barrier for holes vanishes. Consequently, it is advisable to describe the current density in the Schottky junction as the product of a collection velocity v_{coll} , hole concentration $p(z_0)$ at the metallic interface and elementary charge e_0 [11, 12]. This hole collection velocity v_{coll} is the same as the thermionic one, $v_{coll} = \alpha \sqrt{\frac{k_B T}{2\pi m^*}}$, k_B being the Boltzmann constant and α the attenuation coefficient of the reduced thermionic emission due to the oxide interlayer which can be evaluated from the ratio of the effective Richardson constant (see the inset in Fig. 1) to the standard one (96 A/K²cm²) in diamond. This approach remains valid in the depletion regime where $p(z_0)$ is merely the product of the equilibrium hole concentration p_0 in the bulk lightly doped layer and the factor $\exp\left[\frac{-\Phi_B^{hom} + V_j/n}{k_B T}\right]$, but is now essential when $p(z_0)$ deviates in excess from the previous quantity because of the hole injection from the heavily doped layer. Such an effect is firstly evidenced from the deviation existing between experimental data and the full voltage of the $J_p - V$ characteristic taking into account the effect of the 600 Ω series resistance R_s due to the resistivity of the lightly doped layer calculated at room temperature and thermodynamic equilibrium (Fig. 1). The same characteristics simulated with $R_s = 60\Omega$ matches somewhat better the measured points at current densities higher than 10² A/cm² but very badly in the range 1-50 A/cm². This discrepancy shows firstly that the voltage drop in the lightly doped layer is not linear with the current and secondly that it is lower than predicted from the equilibrium

concentration of holes which would induce a 600 Ω series resistance. A even more illuminating property emerges from the plot of the derivative of $J_p - V$, which is nothing other than the specific resistance of the diode, shown in Fig. 2. In this graph, it clearly appears that this specific resistance decreases by a factor larger than ten below $R_s = 600 \Omega$ well before any significant increase of the temperature due to self heating, calculated with a largely overestimated thermal resistance of 100°C/W because of the intimate contact of the rear side of the diamond substrate with the silver heat sink of our sample holder.

In metal/oxide/semiconductor (MOS) heterostructures made on diamond[13], the forbidden bandgap of the oxide is often very similar to that of diamond or it overcomes it by only one or two eV. Consequently, band offsets on oxygenated diamond surfaces are almost systematically close to 1 eV or lower, leaving the thermionic currents over the oxide barrier at an easily detectable level when a sufficient forward polarization is applied. This is the case in our MOS structures consisting of Al on Al₂O₃, 25 nm thick, on a p⁻/p⁺⁺ diamond stack, with an acceptor concentration of 3×10^{17} B/cm³ in the lightly doped layer which is 500 nm thick. Current density-voltage characteristics over a large range of temperatures (103 - 353 K) of such a MOS capacitor are displayed in Fig. 3 as a function of bias voltage applied on the metal electrode. Thermionic current over the barrier of 1.34 eV due to the band offset between the valence band edges[14] and determined like in reference [15] but for an oxygenated diamond surface is responsible for the highest slope in the characteristics. If the current was controlled by the equilibrium concentration of holes at the oxide/diamond interface, it would experience more than fifteen decades of variation over the whole temperature range, relying on a calculation by the formula (1) in [1]. Conversely, current density at a given voltage changes by at most two decades (see Fig. 3), firmly indicating that the hole concentration is not governed by its equilibrium value but rather by a concentration which is strongly dependent of that in the p⁺⁺ layer, practically independent of temperature since diamond is a degenerate semiconductor in this layer. This is the second evidence which demonstrates that current-voltage characteristics in heterostructures comprising a buried heavily doped layer must take hole injection from this p⁺⁺ layer into account.

3 Simulation of the hole transport

In order to check the properties previously evidenced and to gain quantitative insight into the transport mechanisms, simulations and calculations are performed. Firstly, using the finite elements software COMSOL Multiphysics, profiles of the valence band top and quasi-Fermi level of holes are simulated at 300 K in a stack p⁺⁺/p⁻/metal, with a Schottky barrier of 1 V, for applied forward voltages spanning the range 0 to 5 V, each 0.5 V (Fig. 4). The software makes use of all the basic equations which describe semiconductor junctions, as one can find in textbooks like

[16], including both minority and majority carriers transport although the former are unnecessary in the case we are dealing with. The doping concentrations are respectively 2×10^{20} B/cm³ and 10^{15} B/cm³ in the p⁺⁺ and the p⁻ layers, the latter being 2 μm thick. Other boundary conditions are defined on the figure for the electric potentials while the field at the beginning of the p⁺⁺ layer is assumed to be zero because of a perfect ohmic contact, and the carrier velocities at the Schottky contact (at abscissa 2 μm) are given by the product of the mobility [1] and electric field. Saturation of the hole velocity which happens for fields larger than 10^4 V/cm [17] is ignored, involving a shift of the curves in figures 4 and 5 of only a few nanometers toward larger abscissa as estimated from following equations. Depletion regime can be observed close to the metallic interface (at abscissa 2 μm) for applied voltages zero and 0.5 V. But for 1 V and above, band curvature near the metallic interface is inverted and the depletion regime is replaced by accumulation, fully confirming the observations detailed in the previous section. The corresponding hole concentrations are plotted in Fig. 5. Here again, one can see that the hole concentration falls below the equilibrium one $p_0 = 3.5 \times 10^{13}$ cm⁻³ near the Schottky interface for applied voltages zero and 0.5 V, while it increases and stays above and above p_0 for larger and larger voltages. Due to this behavior, it is clear that the voltage drop inside the p⁻ layer can neither follow linearly the current nor be determined by the equilibrium hole concentration p_0 , the real one remaining several times larger up to distances typically near 2 μm from the p⁺⁺ layer boundary.

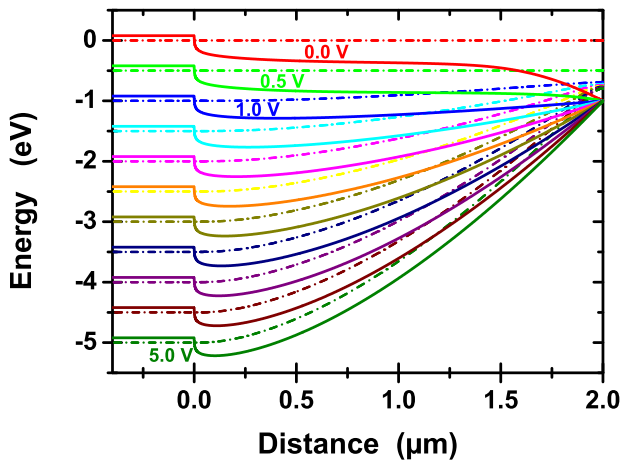


Figure 4 Energy of the valence band top in full lines and quasi-Fermi level of holes in dotted lines, along the depth of a stack p⁺⁺/p⁻/metal measured from the p⁺⁺/p⁻ interface, with a Schottky barrier of 1 eV, for applied forward voltages spanning the range 0 to 5 V, each 0.5 V. Data are obtained from a simulation performed with the software COMSOL Multiphysics for a temperature of 300K. See text for other conditions.

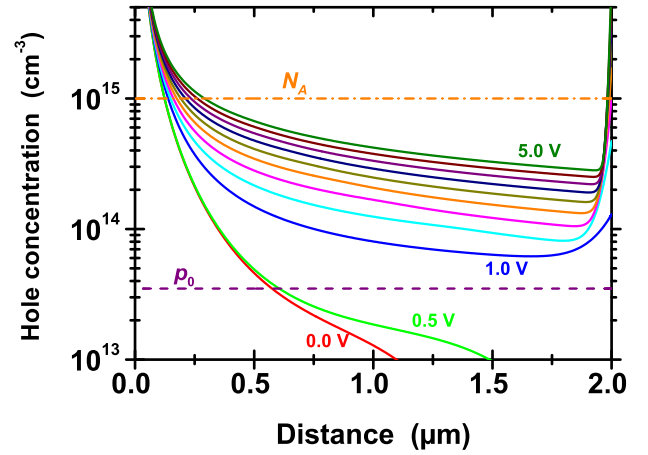


Figure 5 Hole concentration at 300 K as a function of the distance measured from the p⁺⁺/p⁻ interface for forward applied voltages from zero to 5 V, each 0.5 V. The equilibrium hole concentration $p_0 = 3.5 \times 10^{13}$ cm⁻³ and acceptor concentration $N_A = 10^{15}$ cm⁻³ are respectively indicated by dash and dash-dotted lines. Accumulation regime is clearly visible near the Schottky interface, at the 2 μm abscissa.

An other approach relies on usual equations describing transport of charge by majority carriers [16] in the p⁻ layer. Along the z direction, perpendicular to interface, the hole current density equation is the sum of the drift and diffusion components, $\mathcal{E}_z(z)$ being the electric field and $p(z)$ the hole concentration, with $\beta = e_0/k_B T$ and a constant mobility μ_p as previously assumed:

$$J_p = e_0 \mu_p \left[p(z) \mathcal{E}_z(z) - \frac{1}{\beta} \frac{dp(z)}{dz} \right] \quad (1)$$

In accordance with the results of the simulation, the two currents have similar magnitudes but opposite direction close to the origin (p⁺⁺ layer edge) because the very strong diffusion current must be partially compensated by an opposite conduction current so that the constraint imposed by the effective current J_p can be satisfied. Consequently, no terms can be neglected in the previous equation. Moreover, Poisson equation must be satisfied:

$$\frac{d\mathcal{E}_z(z)}{dz} = e_0 [p(z) - N_{ion}^-] / (\epsilon_0 \epsilon_{SC}) \quad (2)$$

where N_{ion}^- is the net, negatively charged, ionized impurity concentration. Elimination of the hole concentration in Eq.(1) with help of Eq.(2) gives the following second order field equation:

$$-\frac{d^2 \mathcal{E}_z(z)}{dz^2} + \beta \mathcal{E}_z(z) \left[\frac{d\mathcal{E}_z(z)}{dz} + \frac{e_0 N_{ion}^-}{\epsilon_0 \epsilon_{SC}} \right] = \frac{\beta J_p}{\epsilon_0 \epsilon_{SC} \mu_p} \quad (3)$$

where the second member is a constant because the current is conservative since there is no recombination. It will be named C in the following.

The two boundary conditions are: (i) $p(0) = p^+$ at $z = 0$, the interface between the heavily and lightly doped layers and p^+ the hole concentration in the heavily doped layer; (ii) at the interface with the metal supposed to be located at $z = z_0$, the carrier collection velocity v_{coll} must be equal to the thermionic one, so that $p(z_0) = J_p/(e_0 v_{coll})$. In terms of the first derivative of the electric field, these two boundary conditions read:

$$(i) \frac{d\mathcal{E}_z(0)}{dz} = \frac{e_0}{\varepsilon_0 \varepsilon_{SC}} [p^+ - N_{ion}^-]$$

and (ii) $\frac{d\mathcal{E}_z(z_0)}{dz} = \frac{e_0}{\varepsilon_0 \varepsilon_{SC}} [J_p/(e_0 v_{coll}) - N_{ion}^-]$.

As we are interested primarily by the extension of the region where the hole concentration largely exceeds the ionized impurity one, the last term of the first member of Eq.(3) is neglected and this equation can then be integrated one time:

$$\frac{e_0}{\varepsilon_0 \varepsilon_{SC}} [p^+ - p(z)] + \frac{\beta}{2} [\mathcal{E}_z(z)^2 - \mathcal{E}_z(0)^2] = Cz \quad (4)$$

Because the concentration $p(z)$ and the square electric field $\mathcal{E}_z(z)^2$ decrease very rapidly from the origin $z = 0$, a good approximation consists to neglect the terms depending on z , so that $\mathcal{E}_z(0)^2 = (2e_0 p^+)/(\beta \varepsilon_0 \varepsilon_{SC})$, resulting in the approximated initial condition : $\mathcal{E}_z(0) = -\sqrt{\frac{2e_0 p^+}{\beta \varepsilon_0 \varepsilon_{SC}}} =$

$\frac{-1}{\beta L_D} \sqrt{\frac{2p^+}{p_0}}$ where L_D is the appropriate Debye length in the lightly doped layer. For other abscissa, the remaining differential equation to be solved reads :

$$\frac{\beta}{2} \mathcal{E}_z(z)^2 - \frac{d\mathcal{E}_z(z)}{dz} = Cz \quad (5)$$

where the first and second terms are respectively due to drift and diffusion components of the current. An exact solution can be found for a vanishing second member, rigorously valid near zero voltage bias: $\mathcal{E}_z(z) = -\frac{2}{\beta} \frac{1}{z+z_1}$ where $z_1 = 2L_D \sqrt{p_0/(2p^+)} = 2\sqrt{\varepsilon_0 \varepsilon_{SC}/(2e_0 \beta p^+)}$ close to 0.3 nm here. This solution shows that the Debye length has still a significance in terms of attenuation distance, despite a non exponential damping law. It still describes satisfactorily the field and hole concentration as long as each of the two terms in the first member of Eq.(5) has a comparable absolute value, much larger than the second member, at abscissa $z < z_c$ of few z_1 . With the help of Eq. (2), one gets $p(z) \approx \frac{2e_0 \varepsilon_{SC}}{e_0 \beta} \frac{1}{(z+z_1)^2}$, which therefore can be retained for the initial hole concentration close to the p^{++} layer till z_c . If $p(z_c) = 2 \times 10^{14} \text{cm}^{-3}$, where z_c is the distance where the hole concentration has dropped from its initial value $p(0)$ by a factor of 10^6 , a fairly good estimate of 0.3 μm is derived, in agreement with the curves plotted in Fig.(5). Beyond such an abscissa, one of the two terms in the first member of Eq.(5) may become dominant and of the same magnitude as Cz . Then, assuming that either the first or the second term can be neglected, solutions based on fractions depending of z

and \sqrt{z} could be found. If only the first term, related to the drift component, is retained, $\mathcal{E}_z(z) \approx \frac{1}{\beta z_2^{3/2}} \sqrt{z+z_1}$ and $p(z) \approx \frac{\varepsilon_0 \varepsilon_{SC}}{e_0 \beta z_2^{3/2}} \frac{1}{\sqrt{z+z_1}}$ can be derived, in agreement with the law given in [5] without justification. But this solution is not correct because the order of magnitude of the constant $z_2 = (2\beta C)^{-1/3}$ makes the second term dominant, contrary to the hypothesis. Similarly, if only the second term, related to the diffusion component, is retained, non physical solutions can be obtained. Such steps show firstly that the drift and diffusion components of the whole hole current remain intimately linked and secondly that Eq.(4) in which the last term of Eq.(3), due to ionized impurities, has been neglected, is no longer appropriate. However, the previous solution obtained for a vanishing second member of Eq.(5) cannot be used because the decrease of the hole concentration would be far too steep in comparison with simulated concentrations in Fig. 5. Consequently, only a numerical solution is able to match the physics of the hole transport in the abscissa range where the hole concentration is close to doping one and decreases in a much softer way. The variation law could resemble better the inverse square root law, leading finally to an estimate of several times z_c for the length where the hole injection affects seriously the equilibrium hole concentration.

A solution valid also near the interface with the Schottky metal or oxide must depend on the current density like what is seen in Fig. 5, or total applied voltage and on boundary conditions at this second interface. It would rely on the same equations using in addition the pseudo-Fermi level of holes $\phi_p(z)$ in $p(z) = N_V \exp[\beta(\phi_p(z) - \Psi(z))]$ and potential $\Psi(z)$, with N_V the effective density of states in the valence band:

$$\frac{d\phi_p(z)}{dz} = -\frac{J_p}{e_0 \mu_p N_V} \exp[\beta(\Psi(z) - \phi_p(z))] \quad (6)$$

$$\frac{d\mathcal{E}(z)}{dz} = \frac{1}{\beta L_D^2} \frac{N_V \exp[\beta(\phi_p(z) - \Psi(z))] - N_{ion}^-}{p_0} \quad (7)$$

$$\frac{d\Psi(z)}{dz} = -\mathcal{E}(z) \quad (8)$$

Boundary conditions must define the differences $\phi_p(z) - \Psi(z)$ at $z = 0$ and $z = z_0$:

(i) $\phi_p(0) - \Psi(0) = (1/\beta) \ln(p^+/N_V)$ and
(ii) $\phi_p(z_0) - \Psi(z_0) = (1/\beta) \ln[J_p/(e_0 v_{coll} N_V) - N_{ion}^-/N_V]$ where $\Psi(z_0)$ can be chosen as the origin of electrical potentials for example. The numerical solver of the COMSOL software solves in fact this set of equations, however taking the current due to minority carriers into account in addition. But because they have a completely negligible influence since the barrier height is much less than half the diamond band gap and no recombination centers are included, the results obtained by an other solver would not be different than those presented at the beginning of this section.

4 Conclusion

In vertical or pseudo vertical Schottky diodes and MOS heterostructures comprising a stack of lightly doped on heavily doped layers, injection of holes play a very significant role in the transport mechanism. Combined with the advent of accumulation regime at sufficiently high forward bias, this effect induce both the decrease of the forward losses and specific resistance when the current density increases, provided the lightly doped layer is less than about $2\ \mu\text{m}$ for doping concentration below $10^{16}\ \text{B}/\text{cm}^3$ like usual for high voltage devices. It allows high current densities higher than $1\ \text{kA}/\text{cm}^2$ under a few volts even at room temperature because the hole concentration in the lightly doped layer becomes largely independent of the temperature, thus alleviating the limitation due to incomplete ionization of acceptors in diamond. However, reverse operation would be preserved with breakdown voltages in the range 1.4 kV to 2 kV as long as breakdown fields in the range 7-10 MV/cm like already achieved[2,6] are implemented in p^- layers 1.4 to $2\ \mu\text{m}$ thick because they are fully depleted and bear the whole reverse voltage. These advantages may have a very positive impact on the performance of high power diamond devices in comparison to components made with other wide bandgap semiconductors.

5 Acknowledgments This work is partially supported by French state funds ANR-10-LABX-51-01 (Labex LANEF du Programme d'Investissements d'Avenir).

References

- [1] Pierre-Nicolas Volpe, Julien Pernot, Pierre Muret, and Franck Omnès. High hole mobility in boron doped diamond for power device applications. *Applied Physics Letters*, 94(9):092102, 2009.
- [2] Pierre-Nicolas Volpe, Pierre Muret, Julien Pernot, Franck Omnès, Tokuyuki Teraji, Yasuo Koide, François Jomard, Dominique Planson, Pierre Brosselard, Nicolas Dheilly, Bertrand Vergne, and Sigo Scharnholz. Extreme dielectric strength in boron doped homoepitaxial diamond. *Applied Physics Letters*, 97(22):223501, 2010.
- [3] Hitoshi Umezawa, Shin ichi Shikata, and Tsuyoshi Funaki. Diamond schottky barrier diode for high-temperature, high-power, and fast switching applications. *Japanese Journal of Applied Physics*, 53:05FP06, 2014.
- [4] V.D. Blank, V.S. Bormashov, S.A. Tarelkin, S.G. Buga, M.S. Kuznetsov, D.V. Teteruk, N.V. Kornilov, S.A. Terentiev, and A.P. Volkov. Power high-voltage and fast response schottky barrier diamond diodes. *Diamond and Related Materials*, in press, 2015.
- [5] Toshiharu Makino, Hiromitsu Kato, Daisuke Takeuchi, Masahiko Ogura, Hideyo Okushi, and Satoshi Yamasaki. Device design of diamond schottky-pn diode for low-loss power electronics. *Japanese Journal of Applied Physics*, 51:090116, 2012.
- [6] A. Traoré, P. Muret, A. Fiori, D. Eon, E. Gheeraert, and J. Pernot. Zr/oxidized diamond interface for high power schottky diodes. *Applied Physics Letters*, 104(5):052105, 2014.
- [7] Pierre Muret, Aboulaye Traoré, Aurélien Maréchal, David Eon, Julien Pernot, Jose Pi nero, M.P. Villar, and Daniel Araujo. Potential barrier heights at metal on oxygen-terminated diamond interfaces; arxiv:1501.04790.
- [8] Jürgen H. Werner and Herbert H. Güttler. Barrier inhomogeneities at schottky contacts. *Journal of Applied Physics*, 69(3):1522–1533, 1991.
- [9] W. Mönch. *Electronic Properties of Semiconductor Interfaces*. Surface Sciences. Springer-Verlag, Berlin Heidelberg, 2004.
- [10] P. K. Baumann and R. J. Nemanich. Electron affinity and schottky barrier height of metaldiamond (100), (111), and (110) interfaces. *Journal of Applied Physics*, 83(4):2072–2082, 1998.
- [11] C R Crowell and S M Sze. Current transport in metal-semiconductor barriers. *Solid-State Electronics*, 9(11-12):1035–1048, 1966.
- [12] E. H. Rhoderick and R. H. Williams. *Metal-Semiconductor Contacts*. Clarendon Press, Oxford, 2nd ed. edition, 1988.
- [13] G Chicot, A Maréchal, R Motte, P Muret, E Gheeraert, and J Pernot. Metal oxide semiconductor structure using oxygen-terminated diamond. *Applied Physics Letters*, 102:242108, 2013.
- [14] A Maréchal, M Aoukar, C Valle, C Rivière, D Eon, J Pernot, and E Gheeraert. Energy-band diagram configuration of alumina/oxygen-terminated p-diamond metal-oxide-semiconductor; submitted.
- [15] J. W. Liu, M. Y. Liao, M. Imura, and Y. Koide. Band offsets of Al_2O_3 and HfO_2 oxides deposited by atomic layer deposition technique on hydrogenated diamond. *Applied Physics Letters*, 101:252108, 2012.
- [16] S. M. Sze. *Physics of Semiconductor Devices*. John Wiley and Sons, New-York, Chichester, Brisbane, Toronto, Singapore, 2nd edition, 1981.
- [17] P. Muret, P.-N. Volpe, T.-N. Tran-Thi, J. Pernot, C. Hoarau, F. Omnès, and T. Teraji. Schottky diode architectures on p-type diamond for fast switching, high forward current density and high breakdown field rectifiers. *Diamond and Related Materials*, 20:285–289, 2011.